Available online at www.sciencedirect.com
SCIENCE DIRECT®
Polymer 44 (2003) 5951–5959
polymer
www.elsevier.com/locate/polymer

Determination of orientation parameters in drawn films of thermotropic liquid crystalline polymer/polypropylene blends using WAXS

Sayant Saengsuwan[a,b], Geoffrey R. Mitchell[b,*], Sauvarop Bualek-Limcharoen[a]

[a]*Department of Chemistry, Faculty of Science, Mahidol University, Rama IV Rd., Bangkok 10400, Thailand*
[b]*Polymer Science Centre, Department of Physics, University of Reading, Whiteknights, Reading RG6 6AF, UK*

Received 25 March 2003; accepted 20 June 2003

Dedicated to Prof. Ian M. Ward on the occasion of his 75th birthday

Abstract

The effects of composition and compatibilizers on the molecular orientation in thermotropic liquid crystalline polymer (TLCP)/PP in situ composite films have been investigated using wide angle X-ray scattering (WAXS) techniques. The degree of preferred orientation for each component was evaluated using a novel separation technique based on a description of the scattering through spherical harmonic functions. The evaluated orientation parameters $\langle P_2 \rangle$ and $\langle P_4 \rangle$ of TLCP phase were found to increase up to 0.76 and 0.53, respectively, with increasing TLCP content and film draw ratio. In contrast, the PP component in all films exhibits a very low orientation ($\langle P_2 \rangle \sim 0.01$) i.e. essentially isotropic. The PP component exhibits the so-called smectic phase which can be transformed to the more stable crystalline phase (α-form) by annealing at 110 °C for 2 h, with a small increase in the level of preferred orientation. The inclusion of particular polystyrene-based compatibilizers was observed to have a substantial effect on the modulus of the composite and in some cases this is reflected in the level of preferred orientation in the TLCP. We deduce that the orientation parameters are largely insensitive to the fibril morphology once a certain aspect ratio has been exceeded.

Keywords: Polypropylene; Liquid crystal polymer; Composite film

1. Introduction

Thermotropic liquid crystalline polymers (TLCPs) can be used to blend with commercial thermoplastic [1–5] in order to achieve composite-like materials with a mechanical reinforcement of the polymer matrix. The presence of small fractions of TLCP in such thermoplastics can reduce their viscosity [6–8] and results in easier processing compared to composites with the solid reinforcements. Most blends of TLCPs and thermoplastics are immiscible. In the molten state, the dispersed TLCP droplets can be elongated under a sufficient shear or extensional force; and after solidification, a TLCP fibrillar morphollogy is formed yielding a so-called in situ composite [1] with enhanced mechanical properties in the fibre orientation direction.

There are many factors affecting the mechanical properties of the blend, not least the fraction and level of preferred orientation of the TLCP phase [3,7,9,10]. For such phase-separated systems, the interaction at the interface is potentially weak, leading to a poor transmission of the mechanical energy from the matrix phase to the reinforcing phase with a resultant premature failure of the material. Therefore, the mechanical properties of these in situ composites are generally lower than those predicted by the Tsai–Halpin's theory [11,12]. Several researchers have attempted to surpass this problem by the addition of compatibilizers in order to reduce the interfacial energy between the matrix and the dispersed phases and hence permit a finer dispersion during mixing [13–15].

The deformation of TLCP droplets into fibrils is strongly influenced by the flow field used during processing. It has been reported that the mechanical properties of the blends with TLCP depend on the level of molecular orientation of TLCP fibre [16–18]. The measurement of the degree of molecular orientation in composite systems poses particular challenges. In this work, we exploit a novel procedure which allows the X-ray scattering recorded for the PP/TLCP

* Corresponding author.
E-mail address: g.r.mitchell@reading.ac.uk (G.R. Mitchell).

0032-3861/03/$ - see front matter © 2003 Elsevier Ltd. All rights reserved.
doi:10.1016/S0032-3861(03)00560-3

composite to be separated in two functions representing the scattering from each of the two constituent phases [19,20]. This approach uses a description of the scattering in terms of a series of Legendre polynomials [21,22] which allows a separation to be made in terms of the orientation and structural contributions to the wide angle X-ray scattering (WAXS) data. The use of these novel WAXS procedures yields, for the first time, the level of molecular orientation and the structure of both the matrix and the dispersed TLCP phase in these in situ composite systems.

In this work, we have used this novel analysis technique the molecular to explore the effects of TLCP content, film-draw ratio and annealing on the orientation parameters of the PP matrix and the TLCP phase. Moreover, the influence of various styrene-based compatibilizers on the orientation parameter of TLCP has also been determined.

2. Experimental

2.1. Materials

The matrix material used in this work was isotactic polypropylene (PRO-FAX 6631) with a melt flow index = 2 g/10 min and T_m = 165 °C, kindly supplied by HMC Co., Thailand. The TLCP (Rodrun LC5000 from Unitika Co. Japan) used as the dispersed phase was a co-polyester of *p*-hydroxy benzoic acid and ethylene terephthalate (80/20 mole ratio) with T_m = 280 °C, and density of 1410 kg/m^3. A series of styrene-based compatibilizers were used in this work, namely, SEBS G1650, SEBS G1652, maleic anhydride grafted SEBS FG1901X (SEBS-g-MA, MW of 4.45×10^4 containing 1.8 wt% MA), and a polystyrene (ethylene–butylene) thermoplastic elastomers (SEP G1701X). SEBS G1650 and G1652 are triblock copolymers of styrene–ethylene–butylene–styrene with a styrene/ethylene–butylene ratio of 29/71 and their number average molecular weight, $\overline{M_n}$, as determined by gel permeation chromatography are 1.05×10^5 and 4.64×10^4, respectively. SEP G1701X is a diblock copolymer of styrene–ethylene–propylene with a styrene/ethylene–propylene ratio of 37/63 and $\overline{M_n}$ of 1.20×10^5. All compatibilizers used in this experiment have a softening point ~180 °C and were kindly provided by Shell Chemical Co.

2.2. Blending and film fabrication

All materials were dried in a vacuum oven at 80 °C for a minimum of 10 h prior to use. PP was melt-blended with 5, 8, 10 and 15 wt% of TLCP. To investigate the effect of the compatibilizers, samples of the 10 wt% TLCP/PP blend were prepared using each of the four types of styrene based compatibilizers of compositions of 1, 3 and 5 wt%. Blending was carried out in a co-rotating intermeshing twin-screw extruder (PRISM TSE-16TC) at a screw speed of 150 rpm. The temperature profile of the extruder is 245/280/285/290/295 °C, representing temperatures at the hopper zone, three barrel zones and the die zone, respectively. Subsequently, the extruded strand was immediately cooled in a water bath and then pelletized. These pellets were again dried in the vacuum oven at 80 °C for at least 8 h in order to remove any moisture. These pellets were fabricated as an extruded thin film using a mini-extruder (Randcastle RCP-0625) equipped with a cast film line. The screw speed used was 70 rpm and the temperature profile was 245/280/290/295 °C, for the hopper zone, two barrel zones and slit die zone, respectively. The gap at the die lip and the width were fixed at 0.65 and 152 mm, respectively. The film exiting from the die outlet was immediately cooled on to a chilled roll and at the same moment was uniaxially drawn at various draw ratios measured as a die gap to film thickness ratio. The films with various draw ratios were prepared in order to verify the relationship between the level of preferred orientation and the draw ratio. Films prepared with the highest draw ratio attained, i.e. 30 (film thickness ~20–22 μm) were used to study the effects of composition on the levels of preferred orientation of the two phases.

2.3. Tensile testing

Tensile testing of the composite films was performed using an Instron mechanical tester (Model 4301) with a gauge length of 25 mm, a crosshead speed of 50 mm/min and a full-scale load cell of 10 N (ASTM D412). Dumbbell-shape specimens were cut from the drawn sheets with the long-axis of the dumbbell parallel to the machine direction (MD) and the results were analyzed using a package program 'Instron IX series'. The results recorded here represent the mean values of at least 10 specimens.

2.4. X-ray measurement

In order to obtain a reasonable X-ray scattering intensity, a thick film (about 0.6–0.9 mm thick) was prepared by folding several layers of the thin film, while maintaining its relative MD direction. The X-ray scattering experiments were performed at room temperature on a 3-circle transmission diffractometer operating in a symmetrical mode which allowed an undistorted map of reciprocal space to be obtained. The scattered intensities were recorded as a function of scattering vector, $|Q|$, varied from 0.2 to 6.0 Å^{-1} in steps of $\Delta Q = 0.02$ Å^{-1} and as a function of azimuthal angle, α, from 0 to 90° in steps of $\Delta\alpha = 9°$ with a count time of 10 s at each position. $|Q|$ is defined as $4\pi \times \sin\theta/\lambda$, where 2θ is the angle between the incident and scattered beam and λ is the incident wavelength of Cu K_α radiation (1.54178 nm). The geometry of the X-ray measurements is presented in Fig. 1. The angle α is measured between the scattering vector Q and the MD of the sample, i.e. $\alpha = 0°$ is the meridional section (parallel to

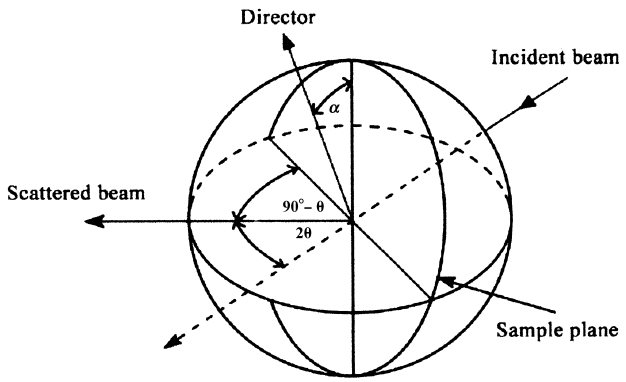

Fig. 1. Illustration of the geometry of 3-circle diffractometer used in this experiment.

the alignment axis or the director axis) and $\alpha = 90°$ is the equatorial section (perpendicular to the alignment axis or the director axis). All data were corrected for absorption, polarization and multiple scattering and scaled to electron units using standard procedures [23].

2.5. X-ray data analysis

The peaks in the scattering patterns for the PP and TLCP components strongly overlap both in terms of $|Q|$ and α and in order to separate the observed scattering data in to that for each component, we have utilized a novel procedure outlined below and more fully described elsewhere [19,20]. For a two phase system in which the morphological scale is very much larger than the molecular separation, the observed scattering can be written as a linear combination of the scattering intensities from each phase:

$$I(Q,\alpha) = xI_{PP}(Q,\alpha) + (1-x)I_{TLCP}(Q,\alpha) \quad (1)$$

where $I(Q,\alpha)$, $I_{PP}(Q,\alpha)$ and $I_{TLCP}(Q,\alpha)$ are the scattering intensities of the composite, neat PP and neat TLCP component, respectively, and x is the fraction of PP. The scattering data for a sample exhibiting uniaxial symmetry can be expressed as a series of spherical harmonic functions [19,22,23]:

$$I(Q,\alpha) = \sum_{0}^{\infty} I_{2n}(Q)P_{2n}(\cos\alpha) \quad (3)$$

where

$$I_{2n}(Q) = (4n+1)\int_0^{\pi/2} I_{2n}(Q,\alpha)P_{2n}(\cos\alpha)\sin\alpha\,\mathrm{d}\,\alpha \quad (4)$$

where P_{2n} are Legendre polynomials; only the even numbered terms are required due to the inversion symmetry inherent in a X-ray diffraction pattern for a non-absorbing sample. Since the observed scattering is a linear combination of the scattering from the two components and the spherical harmonics are orthogonal functions, it follows that the coefficients $I_{2n}(Q)$ of the harmonics of the observed scattering data are also linear combinations of each component. Whereas the 2-d patterns show features which depend on both the spatial structure and the level of preferred orientation, the Q-dependent coefficients of the spherical harmonic functions are only related to the spatial structure. The variation of preferred orientation impacts on each spherical harmonic function through a simple Q-independent scaling factor. As a consequence it is now straightforward to separate the contributions to each spherical harmonic function to those for the PP and TLCP components. This process is particularly facile if the spherical harmonic functions for the pure components are available as they were in this work. This particular approach is based on the spatial correlations being unchanged, but this is easily verified by comparison of the experimental spherical harmonic functions. The 'best-fit' for each set of experimental spherical harmonics is obtained using standard numerical procedures. At each stage the veracity of the procedures was verified by examination of difference functions.

After this separation process, the complete 2-d scattering function for each component may be recalculated from the series of spherical harmonics for that component through Eq. (3). In this work, we utilized the first seven harmonic functions.

Now that scattering has been separated in to its component parts, the data component may be analyzed using conventional procedures in terms of both structure and orientation [23]. In particular, the level of preferred orientation expressed as a series of normalized spherical harmonic coefficients can be obtained through:

$$\langle P_{2n}(\cos\alpha)\rangle^D = \frac{\langle P_{2n}(\cos\alpha)\rangle}{\langle P_{2n}(\cos\alpha)\rangle^m} \quad (5)$$

where $\langle P_{2n}(\cos\alpha)\rangle$

$$= \frac{\int_0^{\pi/2} I^{PP,TLCP}(Q,\alpha)P_{2n}(\cos\alpha)\sin\alpha\cdot\mathrm{d}\,\alpha}{\int_0^{\pi/2} I^{PP,TLCP}(Q,\alpha)\sin\alpha\cdot\mathrm{d}\,\alpha} \quad (6)$$

where $\langle P_{2n}(\cos\alpha)\rangle$ and $\langle P_{2n}(\cos\alpha)\rangle^m$ are the amplitudes of the harmonics belonging to the experimental sample and a model representing perfect alignment, respectively, and $I^{PP,TLCP}(Q,\alpha)$ is either the extracted scattering function for the PP or TLCP components. The terms, $\langle P_{2n}(\cos\alpha)\rangle^D$, represents the orientation distribution function. For $n = 1$, the parameter is the standard Herman's Orientation parameter where $\langle P_2\rangle = 1$ corresponds to perfect alignment and $\langle P_2\rangle = 0$ corresponds to the isotropic case. Analysis of these procedures suggests an uncertainty in the values of the orientation parameters of the order of ± 0.01.

3. Results and discussion

The corrected and scaled 2-d wide-angle X-ray scattering

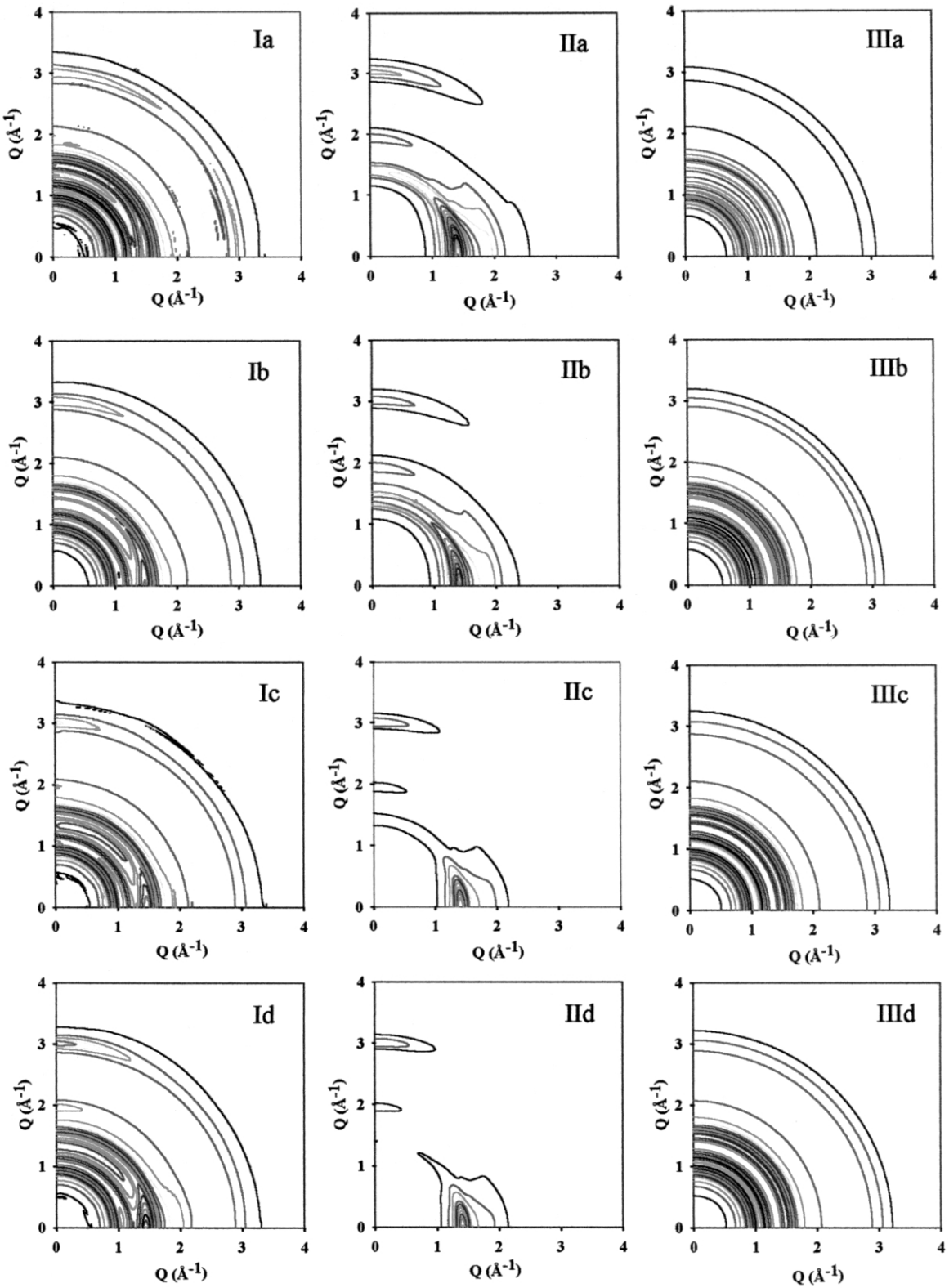

Fig. 2. 2d-scattering patterns of composite films (Column I), extracted TLCP components (Column II) and extracted PP components (Column III): a, b, c and d are the specimen containing 5, 8, 10 and 15wt% TLCP, respectively.

patterns for the 5, 8, 10 and 15 wt% TLCP/PP (draw ratio = 30) samples and their extracted components (TLCP and PP) are shown in Fig. 2. Presented in Column I from top to bottom are the 2-d scattering patterns of 5, 8, 10 and 15 wt% TLCP/PP composites, while in column II and column III are the corresponding extracted TLCP and PP components. The vertical axis in Fig. 2 is the MD or drawing direction of the film. On examination of the scattering data of the composite (Fig. 2, column I), it is not possible to differentiate the contributions from each component, although it is clear that the scattering arises from anisotropic structures. Using the procedure outlined in the previous section, the scattering data were separated in to the component parts. 2-d scattering patterns were then reconstructed from the separated Q-dependent coefficients of the spherical harmonic functions and these are shown in Fig. 2, column II and column III.

It is clear from Fig. 2, that the scattering patterns of the extracted TLCP component show a very high anisotropy, while those of the PP component show a very low anisotropy. There are 3 peaks in the scattering pattern of the reconstructed TLCP (Fig. 2, column II). The first peak is on the equatorial section at $Q = 1.4$ Å^{-1} and arises from intermolecular correlations and thus relates to the spacing between the rod-like structures. The other two peaks are on the meridional section at $Q = 1.98, 3.0$ Å^{-1}. These are associated with intramolecular correlations. These patterns are essentially the same as those reported for the pure TLCP [20–24]. The arc-like characteristics sharpen as the TLCP content increases, indicating an increase in anisotropy. However, the scattering data of the extracted PP components in all specimens (Fig. 2, column III) appeared as ring (halo) patterns implying that the PP phase is more or less isotropic.

Fig. 3 shows plots of the azimuthal sections corresponding to $Q = 1.4$ Å^{-1} for the extracted data for the TLCP component shown in Fig. 2, column II. From the azimuthal

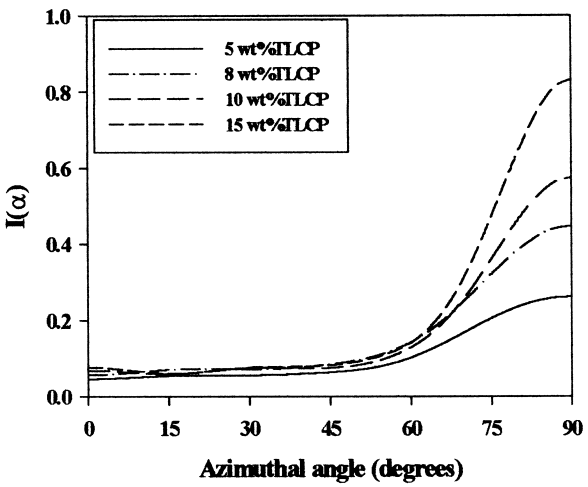

Fig. 3. Azimuthal sections at Q = 1.4 Å^{-1} for extracted TLCP components derived from Fig 2. (Column II).

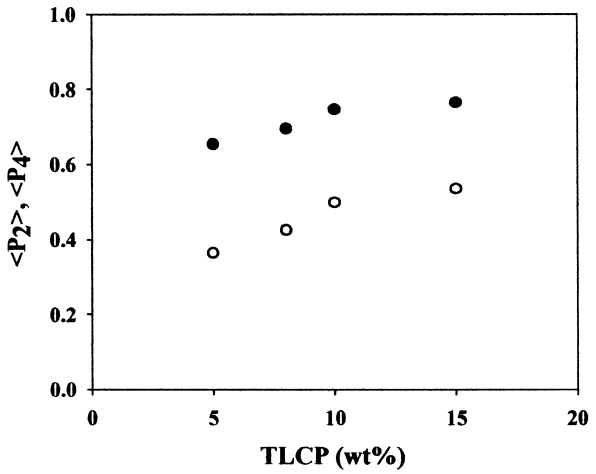

Fig. 4. Illustration of the relationship between $\langle P_2 \rangle$, $\langle P_4 \rangle$ of TLCP component (in the film with draw ratio 30) and TLCP content; ○ and ● represent $\langle P_2 \rangle$ and $\langle P_4 \rangle$, respectively.

profile, the half width, i.e. the width at half maximum peak decreases while the peak intensity increases with increasing TLCP content. This shows that the level of preferred orientation of TLCP components increases with increasing TLCP content. Fig. 4 shows plots of the orientation parameters, $\langle P_2 \rangle$ and $\langle P_4 \rangle$, obtained from analysis of the azimuthal sections shown in Fig. 3 for the TLCP component. As can be seen in Fig. 4, the both orientation parameters increase with an increasing fraction of TLCP, with a trend which appears to level off at compositions greater than 10 wt% TLCP.

Fig. 5 shows the 2-d scattering pattern of a 10 wt% TLCP/PP blend with a draw ratio of 6.5, film thickness ~100 μm, together with its extracted TLCP and PP components. The extracted scattering pattern for the TLCP component (Fig. 5B) displays much larger arc-like patterns, especially centered on the equator at $Q = 1.4$ Å^{-1}, in comparison to the equivalent pattern for the high draw ratio films shown in Fig. 2. The half width at half maximum of the azimuthal section for the extracted TLCP component shown in Fig. 6 is broader than those of all composite films prepared at draw ratio 30, indicating that the degree of preferred orientation decreases with a reduction of film draw ratio. The PP component (Fig. 5C) shows only the same diffuse halo pattern, which indicates that the PP component is almost isotropic similar to the specimen with draw ratio 30.

The effects of the draw ratio on the orientation parameters, $\langle P_2 \rangle$ and $\langle P_4 \rangle$, for 10 wt% TLCP/PP and the compatibilized blend (10 wt% TLCP/PP/3 wt% SEBS G1652) are shown in Fig. 7. A significant increase in the orientation parameter is observed with increasing draw ratio with some tendency to level off at higher draw ratio. The effect of including the compatibiliser in the 10% TLCP blend is marginal in terms of the level of preferred orientation of the TLCP component.

Fig. 8A shows a radial section ($\alpha = 90°$) for the extracted

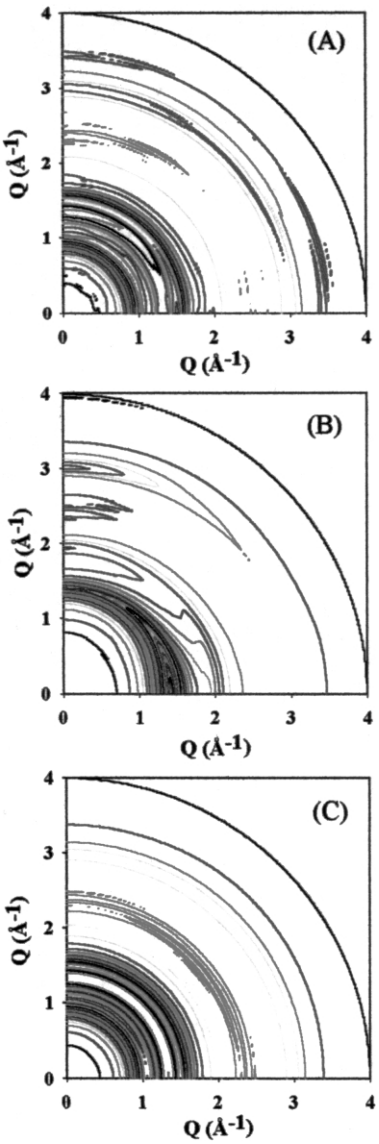

Fig. 5. 2d-scattering patterns of 10 wt% TLCP/PP composite film prepared at draw ratio ~ 6.5 (A) and its extracted TLCP component (B) and PP component (C).

PP component derived from 15 wt% TLCP/PP, draw ratio = 30 sample, which shows three diffuse peaks at Q = 1.04, 1.5 and 3.0 Å^{-1} and also a shoulder at Q = 2.0 Å^{-1}. The azimuthal sections according to the four peaks are presented in Fig. 8B. It is clearly seen that there is little variation in the intensity of those azimuthal scans over the range $\alpha = 0$–90° for the peaks at Q = 1.5, 3.0 and 2.0 Å^{-1}. This means that the PP component is almost isotropic, i.e. random orientation but not completely. Fig. 8C shows a plot of the values of $\langle P_2 \rangle$ for the PP component derived from the series of TLCP/PP composite films prepared with a draw ratio of 30. Although, the values of $\langle P_2 \rangle$ are close to zero, there appears to be a marginal increase of the level of preferred orientation of the PP components with increasing fraction of the TLCP.

Examination of the radial section of the scattering for the

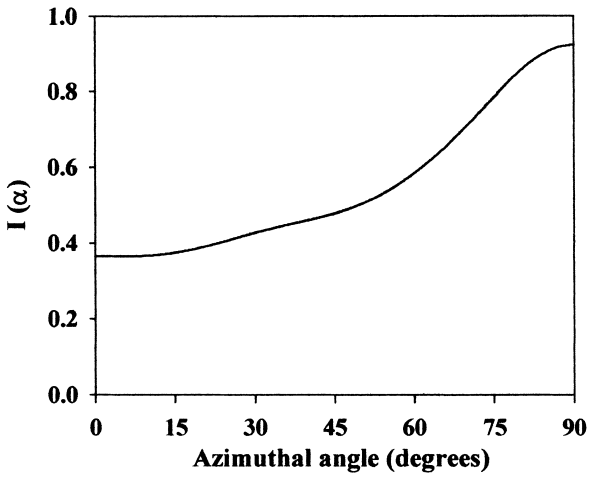

Fig. 6. The azimuthal section of TLCP component at Q = 1.4 Å^{-1} derived from Fig 5(B).

PP component (Fig. 8A) shows that the PP is present in the so-called 'smectic phase' of isotactic PP as first observed by Natta et al. in 1960 [25] and by the later researchers [26,27]. The 'smectic' phase structure is an intermediate state between the crystalline and amorphous phase and consists of parallel chains having a highly conformational ordering

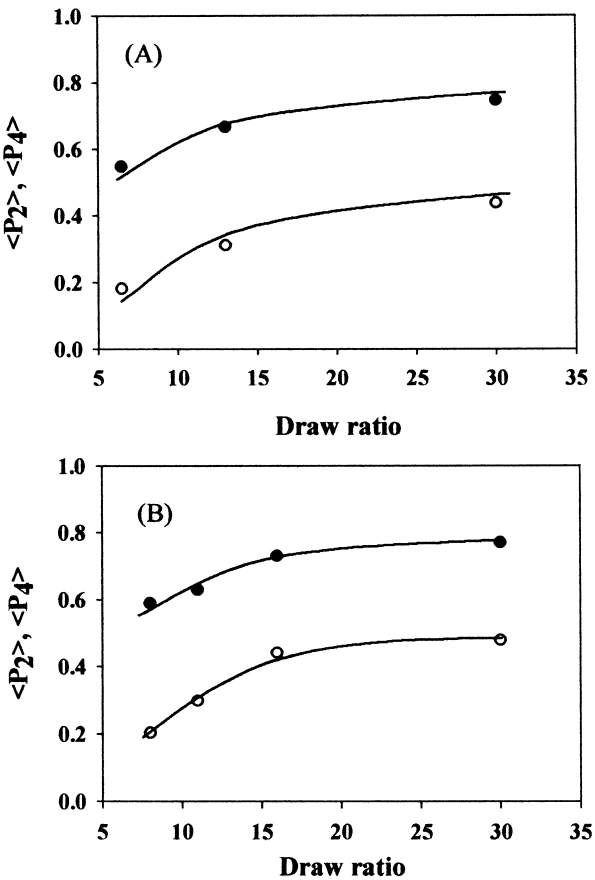

Fig. 7. Plots of orientation parameters $\langle P_2 \rangle$ and $\langle P_4 \rangle$ of the TLCP component versus film draw ratio of 10 wt% TLCP/PP (A) and 10 wt% TLCP/PP/3 wt% SEBS G1652 (B) samples, where ○ and ● represent $\langle P_2 \rangle$ and $\langle P_4 \rangle$, respectively.

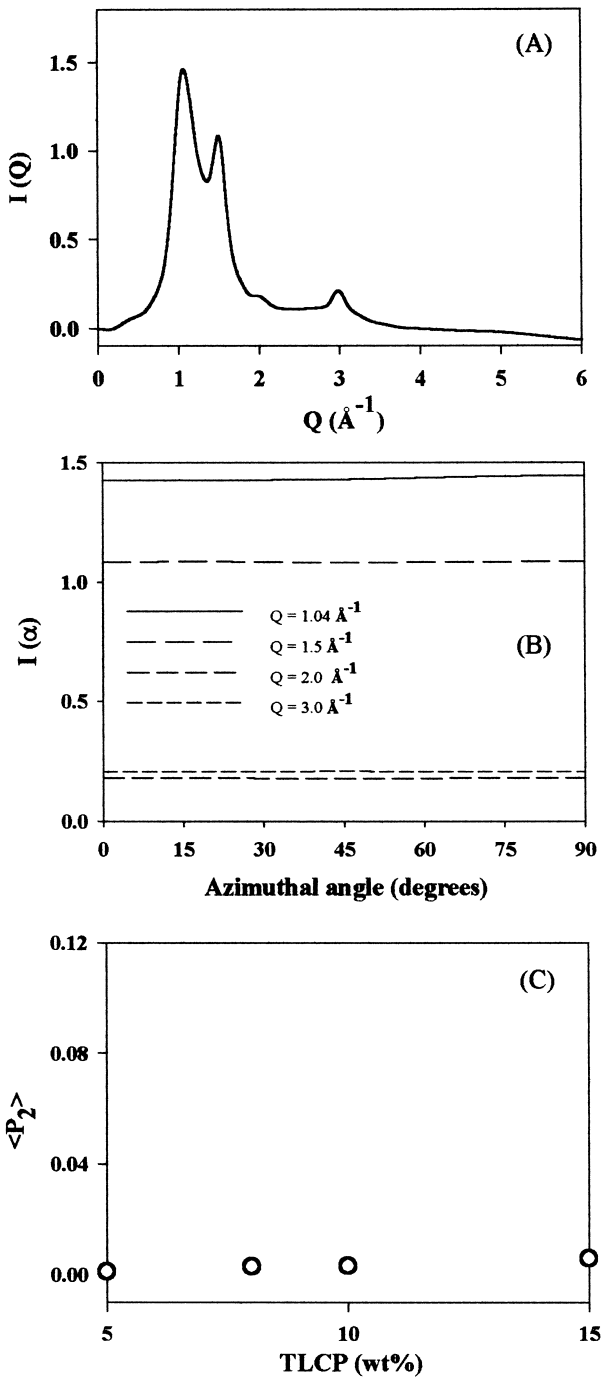

Fig. 8. Equatorial section of extracted component derived from 15 wt% TLCP composite film of draw ratio 30 (A), azimuthal sections of PP corresponding to the four peaks in A (B) and the plot of $\langle P_2 \rangle$ of extracted PP component versus TLCP content (C).

as 3/1 helix, but their lateral arrangements of the helices are rather disordered in comparison to those formed in the monoclinic crystalline phase (α-form). The presence of the 'smectic' phase arises from the rapid cooling which takes place during the final drawing stage. Fig. 9 shows the scattering pattern for a pure PP film prepared under the same conditions and this also shows the 'smectic' phase. The smectic phase of PP can transform to the more crystalline phase (α-form) by means of annealing at appropriate temperature, i.e. 85–150 °C [26]. Fig. 9C shows the scattering pattern for a pure PP film (draw ratio = 30) annealed at 110 °C for 2 h. Fig. 9D shows the equatorial section of Fig. 9C. This scattering pattern confirms that the annealing has resulted in a transformation of the PP to the α-form. By considering the 2-d scattering pattern of annealed PP film (Fig. 9C), it can be seen that the pattern shows a greater level of anisotropy features than that shown in Fig. 9B. This suggests that the transformation is driven more effectively by the portions of 'smectic' PP, which are preferentially aligned with the draw direction. We found that the orientation parameters, $\langle P_2 \rangle$, of as-extruded PP and annealed PP films are about 0.01 and 0.1, respectively. Similar results are obtained for the 15 wt% TLCP/PP composite films after annealing at the same conditions. Fig. 10 shows the scattering extracted for the PP from an annealed TLCP/PP composite film. As with the pure component film there is an apparent increase in the level of $\langle P_2 \rangle$ from ~0.01 to 0.02 on annealing; the order parameter of the TLCP component remains the same ($\langle P_2 \rangle = 0.75$). Of course, the melting point of the TLCP (280 °C) is much higher than the annealing temperature and its solid nature may act as a constraint on the PP. However, it is clear that the transformation from 'smectic' to α-form is particularly selective in that the structures parallel to what was the MD transform grow relative to other orientations.

Table 1 presents the relationship between the Young's modulus of TLCP/PP composite films and the level of preferred orientation of the TLCP component in films of different composition. It is found that the increase of the Young's modulus is in accord with increase in the degree of orientation and the increasing of TLCP content. However, the figures suggest a more complicated relationship since the 15% TLCP sample shows an enhanced modulus in comparison to the trends displayed by the 5–10% range. The level of preferred orientation of the TLCP component reflects the alignment of the fibrils and the director pattern within each fibril. Preliminary microscopy shows that the fibrils are aligned parallel to the draw direction for all draw ratios considered here. Therefore the values of the orientation parameters reflect directly, the director map within each fibril, which in turn will be strongly influenced by the shape of the fibril. In the Tsai–Halpin model of the modulus [11], the critical factor is the aspect ratio of the fibril as well as the moduli of the dispersed and matrix phases. It is unlikely that the enhanced modulus of the 15%TLCP blend can be attributed to an increasing matrix modulus through the marginal increase in anisotropy. Thus the fact that the orientation parameters saturate prior to the modulus values suggests that there are other morphological factors. The most obvious is that the aspect ratio of the fibrils increases continuously with increasing fraction of TLCP through coalescence of the fibrils during extrusion and drawing. Above a certain aspect ratio the level of

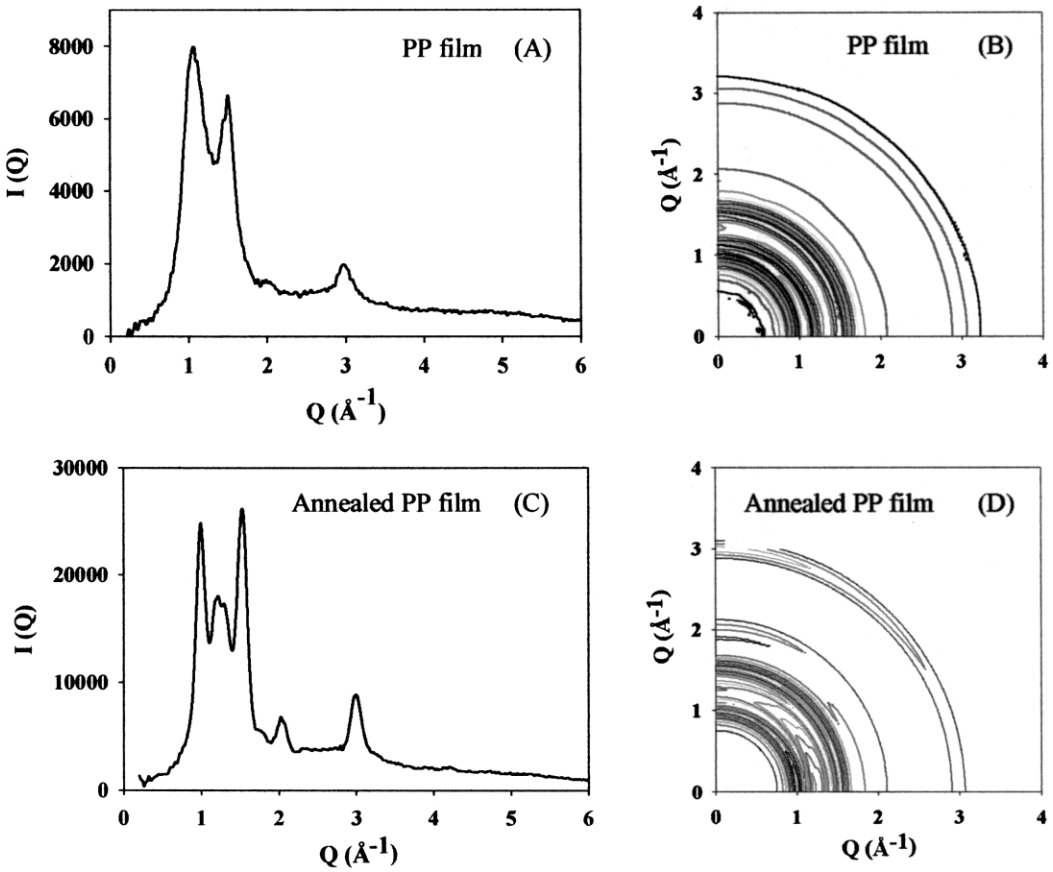

Fig. 9. Comparison of the equatorial sections and 2d-WAXS patterns between PP film (A,B) PP film (C,D) annealed at 110 °C for 2h.

preferred orientation no longer increases as it saturates at the value of the thermodynamic order parameter.

The effects of the type and concentration of compatibilizers on the level of preferred orientation of the TLCP component are also presented in Table 2. There is an overall trend in that the addition of a small fraction (1%) of compatibilizer leads to a reduced modulus and in some cases a reduced orientation parameter. This presumably reflects differing degrees of dispersion of the TLCP with the accompanying changes to the fibril aspect ratio. Whether the reduction in the orientation parameter is significant depends on the scale of the reduction of the aspect ratio. The latter effect is most marked for the di-block and grafted systems in which there is a greater potential for a strong interaction with the TLCP component. Preliminary microscopy observations show that the system with the highest modulus (10% TLCP + 3% SEBS G1652) has the greatest fraction of highly extended fibrils. In essence, the values of the orientation parameter are more influenced by the number of low aspect ratio fibrils than by the specific aspect ratio of highly extended fibrils. Clearly, both orientation and morphological parameters are required for a complete description of these composites. It is clear from the data of Table 2 that the properties of these blends can be significantly affected by the presence of small fractions of compatibilizers, although the addition of fractions >3% appears to be deleterious.

Table 1
Young's modulus of TLCP/PP composites and the order parameters, $\langle P_2 \rangle$, of TLCP component

TLCP content (wt%)	$\langle P_2 \rangle$	Young's modulus (MPa)
5	0.65	945
8	0.69	1069
10	0.75	1183
15	0.76	1706

Table 2
Effect of the type and concentration of compatibilizers on the order parameters, $\langle P_2 \rangle$, of TLCP component in 10 wt% TLCP/PP composite films

Compatibilizer content (wt%)	$\langle P_2 \rangle$			
	SEBS G1650	SEBS G1652	SEBS G1701	SEBS-g-MA
0	0.75	0.75	0.75	0.75
1	0.74	0.76	0.72	0.71
3	0.75	0.77	0.72	0.70
5	0.76	0.76	0.76	0.77

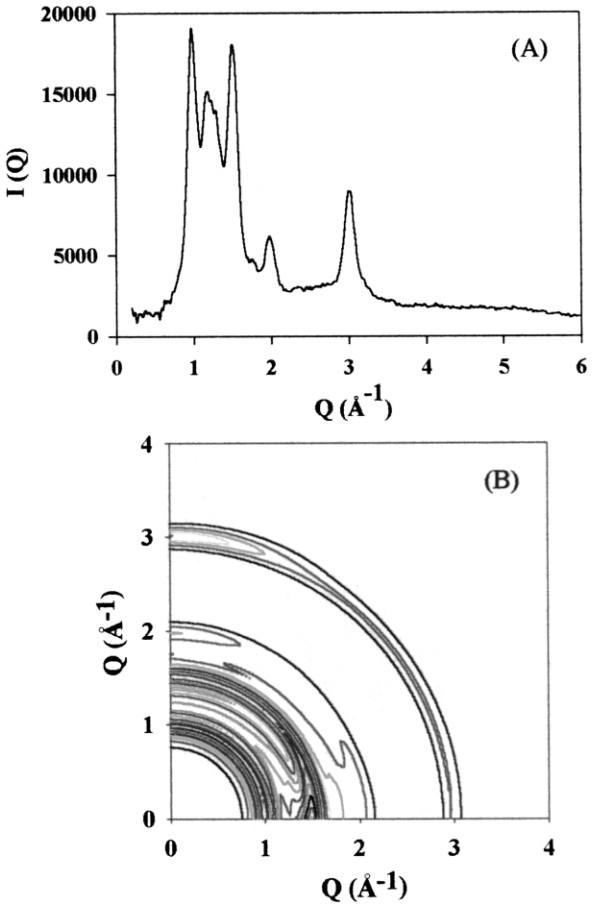

Fig. 10. Equatorial scan (A) and 2d-WAXS pattern (B) for 15wt% TLCP film (draw ratio = 30) annealed at 110 °C for 2h.

4. Conclusions

The novel separation technique based on an analysis in terms of spherical harmonics has been successfully applied to a series of TLCP/PP composites. The overlapping nature of the diffraction maxima for the TLCP and PP components makes separation challenging and the success here suggests that this technique could be usefully applied to other multiphase anisotropic systems. The separation process reveals valuable orientational and structural information about each component. The level of preferred orientation of TLCP component is found to increase with increasing TLCP content and with increasing of the film draw ratio. On the contrary, PP component has $\langle P_2 \rangle$ value around 0.01, which implies that it is nearly isotropic. It is found that the PP phase in both the neat and composite films is in the 'smectic' form, which can be transformed to the more stable α-form by annealing at 110 °C for 2 h. On annealing, the order parameter of PP component is enhanced, while that of the TLCP component is unchanged. The Young's modulus of the composite films in the draw direction increases with increasing level of preferred orientation and TLCP contents. However, there is an enhancement in the improvement of the modulus at the highest fractions of TLCP which suggests some additional morphological factors. It is found that the type and content of compatibilizers has a substantial effect on the modulus and in some cases this is reflected in the level of preferred orientation of the TLCP component.

Acknowledgements

Financial support by the Royal Golden Jubilee Program (PHD/00047/2541), Thailand Research Fund and the Postgraduate Education and Research program in Chemistry (PERCH) are gratefully acknowledged.

References

[1] Kiss G. Polym Sci Engng 1987;27(6):410–23.
[2] Datta D, Fruitwala H, Kohli A, Weiss RA. Polym Sci Engng 1990;30:1005–18.
[3] Handlos AA, Baird DGB. JMS Rev Macromol Chem Phys 1995;C35:183.
[4] Qin Y. Polym Adv Tech 1995;7:151–9.
[5] Aciernio D, Collyer AA, editors. Rheology and processing of liquid crystalline polymers. London: Chapman and Hall; 1996.
[6] Heino MT, Hietaoja PT, Seppala JV. J Appl Polym Sci 1994;51:259–70.
[7] He J, Bu W, Zhang H. Polym Engng Sci 1995;35(21):1695–704.
[8] Bualek-Limcharoen S, Saengsuwan S, Amornsakchai T, Wanno B. Macromol Symp 2001;170:189–96.
[9] Zhuang P, Kyu T, White JL. Polym Engng Sci 1988;28(17):1095–106.
[10] Nielsen LE. Mechanical properties of polymers and composites, II. New York: Marcel Dekker; 1974.
[11] Halpin JC, Kardos JL. Polym Engng Sci 1976;16:344.
[12] Crevecoeur G, Groeninckx G. Polym Engng Sci 1990;38(9):532–42.
[13] Datta A, Chen HH, Baird DG. Polymer 1993;34:759–66.
[14] Kozlowski M, Mantia FPL. J Appl Polym Sci 1997;66:969–80.
[15] Bualek-Limcharoen S, Samran S, Amornsakchai T, Meesiri W. Polym Engng Sci 1999;39(2):312–20.
[16] Ajji A, Brisson J, Qu Y. J Polym Sci, B 1992;30:505–16.
[17] Lin Q, Jho J, Yee AF. Polym Engng Sci 1993;33(13):789–98.
[18] Nakinpong T, Bualek-Limcharoen S, Bhutton A, Aungsupravate O, Amornsakchai T. J Appl Polym Sci 2002;84(3):561–7.
[19] Mitchell GR, Saengsuwan S, Bualek-Limcharoen S. Polym Preprint 2002;43:197–8.
[20] Mitchell GR, Saengsuwan S, Bualek-Limcharoen S. J Appl Crystallogr. Submitted for publication.
[21] Mitchell GR, Windle AH. Polymer 1982;23:1269–72.
[22] Mitchell GR, Windle AH. In: Bassett DC, editor. Developments in crystalline polymers-2. London: Elsevier; 1988. p. 115–75.
[23] Mitchell GR. X-ray Scattering from non-crystalline polymers. In: Allen G, Bevigton J, editors. Comprehensive polymer science. New York: Pergamon Press; 1988. p. 687–729.
[24] Nakamae K, Nishino T, Kuroki T. Polymer 1995;36(14):2681–4.
[25] Natta G, Corradini P. Nuovo Cimento Suppl 1960;15:40–51.
[26] Seguela R, Staniek E, Escaig B, Bertrand Fillon B. J Appl Polym Sci 1999;71:1873–85.
[27] Cohen Y, Saraf RF. Polymer 2001;42:5865–70.